

Binaries among low-mass stars in nearby young moving groups [★]

Markus Janson¹, Stephen Durkan², Stefan Hippler³, Xiaolin Dai³, Wolfgang Brandner³, Joshua Schlieder⁴,
Mickaël Bonnefoy⁵, and Thomas Henning³

¹ Department of Astronomy, Stockholm University, Stockholm, Sweden

e-mail: markus.janson@astro.su.se

² Astrophysics Research Center, Queens University Belfast, Belfast, Northern Ireland, UK

e-mail: sdurkan01@qub.ac.uk

³ Max Planck Institute for Astronomy, Heidelberg, Germany

e-mail: hippler@mpia.de, xiaolin@mpia.de, brandner@mpia.de, henning@mpia.de

⁴ NASA Exoplanet Science Institute, Caltech, Pasadena, California, USA

e-mail: jschlied@ipac.caltech.edu

⁵ Univ. Grenoble Alpes, IPAG, Grenoble, France

e-mail: mickael.bonnefoy@univ-grenoble-alpes.fr

Received —; accepted —

ABSTRACT

The solar galactic neighbourhood contains a number of young co-moving associations of stars (so-called ‘young moving groups’) with ages of ~ 10 –150 Myr, which are prime targets for a range of scientific studies, including direct imaging planet searches. The late-type stellar population of such groups still remain in their pre-main sequence phase, and are thus well suited for purposes such as isochronal dating. Close binaries are particularly useful in this regard, since they allow for a model-independent dynamical mass determination. Here we present a dedicated effort to identify new close binaries in nearby young moving groups, through high-resolution imaging with the AstraLux Sur Lucky Imaging camera. We surveyed 181 targets, resulting in the detection of 61 companions or candidates, of which 38 are new discoveries. An interesting example of such a case is 2MASS J00302572-6236015 AB, which is a high-probability member of the Tucana-Horologium moving group, and has an estimated orbital period of less than 10 years. Among the previously known objects is a serendipitous detection of the deuterium burning boundary circumbinary companion 2MASS J01033563-5515561 (AB)b in the z' -band, thereby extending the spectral coverage for this object down to near-visible wavelengths.

Key words. Binaries: visual – Stars: low-mass – Stars: pre-main sequence

1. Introduction

Young Moving Groups (YMGs) are associations of stars that, in addition to having individual indications of youth, are clustered in phase space and therefore generally assumed to originate from a common birth cluster (e.g. Torres et al., 2000; Zuckerman et al., 2001). Thus, they can be expected to be approximately co-eval, which opens up for a range of scientific opportunities that are otherwise unattainable. For instance, statistical age estimators can be applied to a large number of stars in a YMG in order to average out the scatter and improve the precision of the age, and conversely, if the age of individual stars can be determined with particularly good accuracy, this can feed back to the age estimation of all other stars that are associated with the same YMG. The age is a fundamental parameter for many purposes in stellar science, but one of the main reasons for why it has received particular attention in recent years is its relevance for exoplanet research. Since planets are maximally hot directly after formation and subsequently cool gradually for the rest of their lifetime (or until they reach a thermal equilibrium

due to illumination from a parent star), the interpretation of a directly imaged planet depends crucially on understanding its age (e.g. Marois et al., 2008; Lagrange et al., 2010; Kuzuhara et al., 2013). Since YMGs are additionally prime targets for direct imaging surveys due to their youth and proximity (e.g. Chauvin et al., 2010; Biller et al., 2013; Brandt et al., 2014), understanding the ages of YMGs is intimately coupled to the understanding of directly imaged planets.

M-type stars have rather long pre-main sequence lifetimes of ~ 100 Myr (e.g. Baraffe et al., 1998). As a result, when such stars reside in YMGs, they are typically still evolving through the pre-main sequence phase, and thus they can potentially be isochronally dated to a good level of precision. Such isochronal dating can in principle be performed using a T_{eff} versus L_{bol} relationship (e.g. Janson et al., 2007), but the temperature scale of M-dwarfs is highly uncertain and thus a potential cause of systematic error. A more robust analysis can be based on using an M_{star} versus L_{bol} relationship instead. This has been achieved in a few cases (e.g. Bonnefoy et al., 2009; Köhler et al., 2013; Montet et al., 2015a), but more examples would be highly beneficial for covering more YMGs and more reference cases in each YMG to test for robustness, co-evality within YMGs, etc. In previous high-resolution imag-

Send offprint requests to: Markus Janson

[★] Based on observations collected at the European Southern Observatory, Chile (Programs 096.C-0243 and 097.C-0135).

ing surveys, we have identified a large number of binaries in young systems (Bergfors et al., 2010; Janson et al., 2012a). However, not all of these can be associated to known YMGs, and only a subset of the discovered binaries have orbital periods that are short enough so that robust orbital parameters can be estimated in a reasonably rapid timeframe (Janson et al., 2014a). In order to increase the yield of high-utility binaries, it would be most efficient to target stars that have already been identified as YMG members.

Here, we present the results of a high-resolution imaging survey of low-mass stars that have been identified as probable members of nearby YMGs (Malo et al., 2013, 2014; Kraus et al., 2014), primarily motivated by the reasoning above. In the following, we will first present the selected sample of stars in Sect. 2 and the acquisition and reduction of the imaging data in Sect. 3. We will then discuss the results for the sample at large in Sect. 4.1, pay special attention to the ‘planetary mass’ companion 2MASS J01033563-5515561(AB)b in Sect. 4.2 and note peculiarities of other targets in Sect. 4.3. Finally, we will summarize the results of the survey in Sect. 5.

2. Target sample

Our targets were selected from three catalogues of late-type stars identified as high-probability members of nearby YMGs (Malo et al., 2013, 2014; Kraus et al., 2014) that had not been previously monitored with AstraLux. In principle, six observational parameters are required to exactly relate the *XYZUVW* of the target to that of various moving groups it could conceivably be associated to, but since late-type stars are faint at visible-light wavelengths, most potential YMG members lack a parallactic distance, and many lack a radial velocity measurement, so a probabilistic estimation must sometimes be made on the basis of only four parameters (right ascension, declination, and proper motion along both these directions). Nonetheless, the Bayesian estimations made in e.g. Malo et al. (2014) using the so-called BANYAN code can often distinguish field objects from moving group members with such a constrained parameter set with quite high probabilities, provided that the priors are trustworthy.

For the purpose of scheduling and executing the observations, we took the membership assignments in the aforementioned catalogues at face value. However, since then, the first *Gaia* data release has been presented (Brown et al., 2016), including the Tycho-Gaia Astrometric Solution (TGAS, see Michalik et al., 2015). This contains new parallaxes and improved proper motions for 29 of the observed targets. Hence, for these cases we re-evaluated YMG membership using the BANYAN II tool (Gagné et al., 2014) with the updated astrometry from *Gaia*. In many cases, the *Gaia* parallactic distance was remarkably close to the kinematic distance prediction yielded by BANYAN when no measured parallax is provided. Some particularly notable cases are mentioned in Sect. 4.3. In this way, we found that the YMG membership hypothesis is supported (and strengthened) with the addition of a *Gaia* parallax in 17 of the 29 cases. However, in the other 12 cases, membership could not be supported, with the YMG probability going down to effectively 0% in some cases. This relatively high rejection rate should be taken as a caution that the other targets, for which no parallactic distance exists yet, should still be taken only as candidate YMG

members, rather than bona fide members. Still, the fact that a majority of the re-assessed cases were verified as YMG members can be seen as an indication that most of the other candidate assignments are probably also correct. In due time, *Gaia* will provide accurate distances to all of these targets, such that membership can be more robustly assessed across the board.

The sample properties are listed in Table 1.

3. Observations and Data Reduction

The observations of this survey were taken during three separate runs during the European Southern Observatories (ESO) observing periods P96 (program 096.C-0243) and P97 (program 097.C-0135). Two of the runs were scheduled in P96, with four nights spanning 24–27 Nov 2015 and another four nights spanning 24–27 Dec 2015. Unfortunately, the Nov run suffered from very poor conditions with clouds, strong winds, and poor seeing, so only a few targets could be usefully observed for the survey on the night of Nov 27. The Dec run was considerably better and yielded useful data every night. In P97, the single four-night run was scheduled for 16–19 May 2016. One of these nights, May 17, was very productive and offered a clear sky and good seeing for most of the night, but like in the Nov run, the rest of the time was clouded out.

For all of the observations, we used the AstraLux Sur Lucky Imaging camera (Hippler et al., 2009) mounted at the guest instrument port of the 3.5m New Technology Telescope (NTT) in La Silla. The z' filter was used, and typically 10000 frames with individual integration times of a few tens of ms were acquired for each target. In total, we observed 181 separate targets during the available clear nights. Nine of these were observed twice, since some of the binary candidates detected in the late 2015 runs were re-observed in the May 2016 run. Generally, a subarray read-out of 256×256 pixels was used since we are primarily interested in close binaries, but in the case of wide binaries, where both components may be interesting or where it was not immediately obvious to the observer which star was the actual target, the full 512×512 detector was read out in order to maintain both components firmly within the field of view. The field of view for the full frame is approximately $16'' \times 16''$.

Data reduction was done in an identical way to our previous AstraLux surveys (e.g. Janson et al., 2012a, 2014a). The reduction pipeline (Hormuth et al., 2008) produces several Lucky Imaging outputs with different levels of selection (e.g. all frames used, the 10% best seeing frames used, the 1% best seeing frames used etc). For our purposes, we consistently chose a 10% selection for further analysis as it provides a good trade-off between resolution and sensitivity. The final pixel scale as well as the True North orientation were determined individually for the different runs by observing clusters that have been previously observed with the Hubble Space Telescope (HST) for astrometric reference. For the Nov 2015 and Dec 2015 runs, we used Trapezium for this purpose with HST coordinates from McCaughrean et al. (1994), and for the May 2016 run, we used M15 with HST coordinates from van der Marel et al. (2002). In this way, we found pixel scales of 15.19 mas/pixel for the Nov 2015 run, 15.20 mas/pixel for the Dec 2015 run, and 15.27 mas/pixel for the May 2016 run. Likewise, we derived True North orientations of 2.17 deg for Nov 2015, 2.40

deg for Dec 2015, and 3.04 deg for May 2016. The calibration uncertainties range 0.06–0.13 mas/pixel in pixel scale and 0.16–0.30 deg in True North orientation.

From the output images, relative astrometry and photometry was derived for any pair of stars that could be identified in the images. This was again done as in our previous studies, with aperture photometry and Gaussian centroiding in the case of wide separation pairs, and Point Spread Function (PSF) fitting for close separation pairs, where the PSFs of single stars were used as references. Triple systems consisting of a close pair and a third wide component need special attention in this regard. We handled these by choosing an aperture large enough to encompass both components of the close pair, thus acquiring an AB–C (or A–BC) relative photometry. The relative photometry of the close pair was then determined through PSF fitting as usual, and from this the relative photometry between the brighter component of the pair and the wider component could be derived. Near-equal brightness pairs are subject to the so-called ‘false triple’ effect (Law, 2006), in which the pair of components map onto three apparent PSFs in the final image, also require special attention. In the context of astrometry, there is a 180 deg ambiguity in the position angle of such cases, since it cannot be uniquely determined which is which of the two binary components (this is an issue for nearly equal-brightness components even in the absence of a false triple effect). In the context of photometry, we have shown in previous papers (Janson et al., 2012a, 2014b) that the photometric determinations on false triple pairs are biased, hence for this study, we simply omit a relative photometric analysis of such systems.

4. Results and discussion

4.1. Multiplicity in the sample

Among our sample of 181 targets, we detect 61 candidate companions, of which 23 have been previously reported in the Washington Double Star catalogue (Mason et al., 2001) and other sources cited individually in this article. The other 38 are, to our knowledge, new detections. An example of the new detections, the triple system J17243644-3152484, is shown in Fig. 1.

The astrometric properties of the multiple systems are summarized in Table 2. Of the 23 companions that have been previously observed, each one could be confirmed to share a common proper motion (CPM) with the primary. This is consistent with our experience from previous surveys (e.g. Janson et al., 2012a), that the contamination frequency is low for typical targets (i.e., targets that are not very close to the galactic plane). While we do have second epoch observations for nine companions of which eight are new, the proper motions for several of them are too small to be statistically significantly measurable over a ~ 5 month baseline. J12092998-7505400 AB could nonetheless be confirmed as CPM with $>10\sigma$ confidence. While not yet formally noted as CPM in the table, J07343426-2401353 AB and J07523324-6436308 BC could be seen as marginally confirmed CPM at 3–4 σ . For the targets that neither have literature epochs nor could be confirmed as CPM, we made an additional test by checking digital sky surveys for historical epochs for the targets. This is similar to the checks performed in Janson et al. (2014b), as well as in other recent surveys (e.g. Montet et al., 2015b; Schlieder et al., 2016).

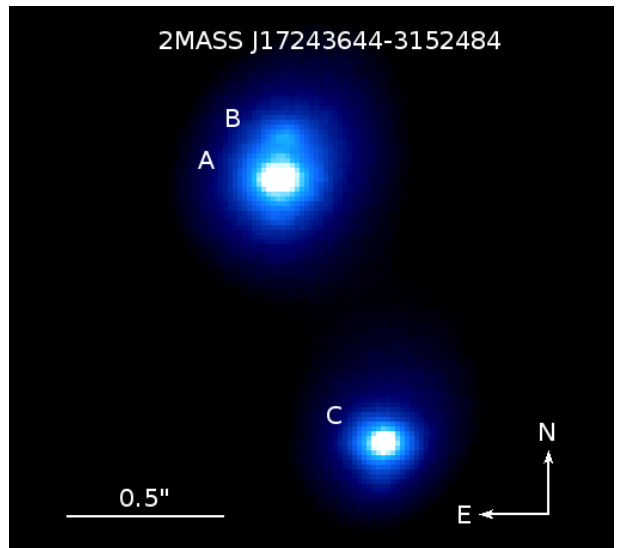


Fig. 1. Image of the J17243644-3152484 triple system, resolved by AstraLux for the first time. The YMG classification of this system is unclear, as discussed in Sect. 4.3.

The best source for such checks is typically the Palomar Observatory Sky Survey (POSS), which includes images covering a large fraction of the sky from epochs around 1950, thus providing a sufficient baseline for targets with proper motions of ~ 100 mas/yr to move by several arcseconds on the sky, which is usually more than the seeing-limited resolution of the images. Thus, background contaminants in the AstraLux image may be separated from the primary in such archival images for sufficiently fast-moving targets. Unfortunately, most of our targets are too far south to be included in POSS. In these cases, the best option is typically the so-called SERC survey from the UK Schmidt telescope, which has first epoch data from typically the late 1970s or early 1980s. Furthermore, some of our targets with candidate companions have a quite slow proper motion, down to 11 mas/yr in the slowest case. In order to be able to draw confident conclusions, we set the threshold that 3'' of motion must have occurred between the archival epoch and the AstraLux data for the archival epoch to be useful. This leaves 15 targets that can be usefully checked. Of these, there are 10 cases in which no candidate background star can be seen in the archival image. This strongly implies that the respective candidates are physical companions. In this context it should still be considered that the filters of the two epochs are quite different; the archival epochs are at shorter wavelengths than the AstraLux data. Hence, a hypothetical very red background source may escape detection in the archival data, in which case it would be erroneous to label the candidate as CPM. We consider that a positive detection is needed for a final confirmation of CPM, and thus we label these candidates as ‘implied CPM’ rather than fully confirmed CPM. This is marked with the label ‘I’ in Table 2. In the remaining five cases, the separation between the primary and candidate was large enough that they could be recognized as partially resolved in the archival images, such that a real CPM test could be performed. In this way, we could confirm three additional CPM companions (J00302572-6236015 C, J18450097-1409053 B, and J23204705-6723209 B), and two background contaminants (J00514081-5913320 B and J23332198-1240072 B).

The relatively large rejection fraction is due to the fact that these are the widest among the candidates, which is where the contaminants are expected to reside. Of the candidates that remain unverified, we expect that three (J05111098-4903597 B and J16572029-5343316 B and C) are possible/probable background contaminants, but the rest are very close and/or very bright relative to the primary, hence they are all probable companions. Obviously, common proper motion tests over a longer timescale will be required to verify this beyond reasonable doubt in the individual cases.

Photometry and derived quantities are shown in Table 3. The relative photometry was used to estimate individual masses using theoretical mass-luminosity relationships for young stars. Each target system was assigned an age based on their YMG membership assignment as shown in Table 1. The ages for the AB Dor (ABMG, ~ 150 Myr), β Pic (bPMG, ~ 25 Myr), Carina (CAR, ~ 45 Myr), Columba (COL, ~ 40 Myr), Tucana-Horologium (THA, ~ 45 Myr) and TW Hya (TWA, ~ 10 Myr) YMGs were adopted from Bell et al. (2015). Argus is considered a questionable association by Bell et al. (2015), but is used in the BANYAN framework, so we assign it an age of 40 Myr following Torres et al. (2008). For a given star with a given age, we adopt the evolutionary models of Baraffe et al. (2015) to make predictions of the masses from the measured brightnesses. The combination of masses for the two components of a binary pair that minimizes the RMS residuals of the $\Delta z'$ from our data and the total J -band magnitude from 2MASS (Skrutskie et al., 2006) is adopted for this purpose. The total mass m_{tot} of the binary in combination with an estimated semi-major axis a can then in turn be used to make a tentative prediction for the orbital period P of the pair, since $P \sim m_{\text{tot}}^{-1/2} a^{3/2}$. An estimation for the semi-major axis can be acquired simply by considering that for sensible eccentricity distributions, the ratio between average projected separation and semi-major axis of a binary population is close to unity (Brandeker et al., 2006; Bonavita et al., 2016). In other words, the expectation value for the semi-major axis of a binary with no additional information about its orbit is approximately equal to its instantaneous projected separation. The period estimations resulting from this analysis are shown in Table 3. These estimations are subject to large uncertainties, for a range of reasons such as systematic uncertainties in the models and ages, as well as the broad scatter in the translation between projected separation and semi-major axis. However, prior to measuring the actual orbits, this is the best that can be done with the data at hand, so it is a useful procedure for determining which systems are the most promising to follow up with a relatively high cadence for an orbital determination within a realistic timescale. Indeed, identifying such systems is the primary purpose of this study.

As mentioned previously, the false triple binaries are unsuitable for relative photometry and thus not included in Table 3, but it is still of interest to acquire approximate period estimations. For this purpose, we apply a simplified procedure of assuming that the components are approximately equal brightness, and estimate the mass based on total J -band magnitude alone. Through this procedure, we acquire estimations of 8 yr for J00302572-6236015 AB, 43 yr for J01033563-5515561 AB, 9 yr for J02303239-

4342232 AB, 295 yr for J04475779-5035200 AB, 111 yr for J12092998-7505400 AB, 89 yr for J17130733-8552105 AB, 39 yr for J20223306-2927499 AB, and 91 yr for J21342935-1840372 AB. In total among the pairs studied in this survey, this means that 9 pairs have an estimated orbital period < 40 years, which we deem as the relevant cut-off timescale for sufficiently rapid orbits to motivate regular astrometric monitoring. We particularly note the two pairs J00302572-6236015 AB and J02303239-4342232 AB, which both have very rapid estimated orbital timescales of < 10 years. J00302572-6236015 is identified as a THA member in Kraus et al. (2014), and a BANYAN II check supports this at a very high level of probability (99.7% THA member with standard priors), though a parallax distance is still required for it to formally be regarded as a bona fide member. J02303239-4342232 has been extensively studied in a YMG context (e.g. Torres et al., 2008; Schlieder et al., 2010); in this study our baseline YMG assumption was based on the COL classification in Malo et al. (2014). Since then, a parallax has become available in TGAS which we could use to verify this membership in a BANYAN II analysis. We find that with standard priors, the probability of COL membership is 82.6%, with a small alternative probability of 15.2% that it is a member of THA instead. The probability of it being a field contaminant is only 1.9%. In other words, it is very likely to be a genuine YMG member. We therefore consider J00302572-6236015 AB and J02303239-4342232 AB to be the very top priorities for astrometric follow-up out of the 61 examined in this work.

4.2. The case of 2M0103

An interesting ancillary outcome of our survey was the re-detection of J01033563-5515561(AB)b (system identifier hereafter abbreviated as 2M0103) originally reported in Delorme et al. (2013). Our image, which is displayed with a high stretch and has been smoothed with a Gaussian kernel of 20 pixel (304 mas) FWHM, can be seen in Fig. 2. 2M0103(AB)b was estimated in Delorme et al. (2013) to be a ~ 12 – $14 M_{\text{jup}}$ object at a relatively wide orbit (~ 84 AU projected separation) around a close low-mass stellar binary pair. It can therefore in some sense be regarded as a possible circumbinary planet, although it seems unlikely that it would have formed through standard planet formation mechanisms, at least at its present location. The targets of our survey were selected solely on the basis of probable late-type YMG members that had not previously been observed by AstraLux, hence the inclusion of this target in the survey was entirely coincidental. Only after we had discovered the point source in the AstraLux images, and a detailed literature search was made for 2M0103, was the history of the system realized.

Special considerations are required to constrain the properties of 2M0103(AB)b, because the conditions were non-optimal during the observation and the companion is faint and embedded in the PSF halo of the central binary, and also because the central binary exhibits a false triple effect, further complicating matters. We estimate relative photometry by using 15 pixel circular apertures around the primary pair and around the faint companion. The contribution of the PSF halo of the primary pair was estimated by taking the mean of the aperture flux at four different locations at the same separation from the pair as

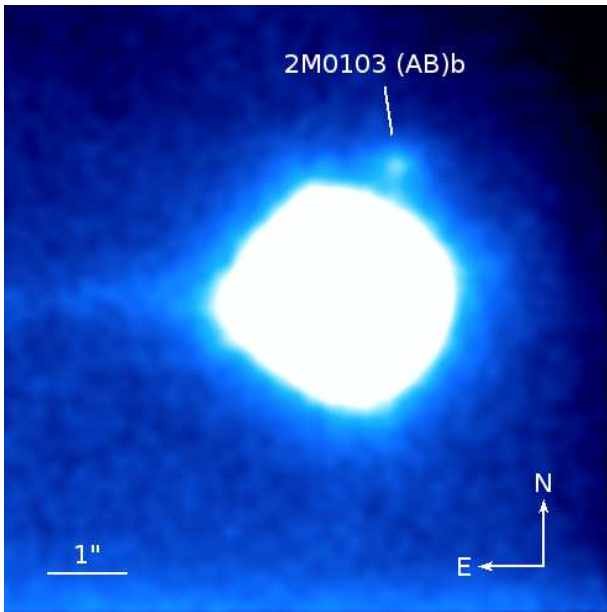


Fig. 2. Astralux z' image of the 2M0103 system. Smoothing with a Gaussian kernel has been applied to better show the faint very low-mass companion first reported in Delorme et al. (2013).

the companion. The points chosen for this purpose were due North, South, and West from the primary pair, as well as the point directly opposite to the companion’s location. The Eastward direction was omitted for this purpose, since the PSF halo has a coma-like extension in that direction. In this way, we found that the AB–b contrast is $\Delta z' = 6.5 \pm 0.3$ mag. This is the only photometric quantity that is directly measurable in the data due to the false triple effect of the primary, but if we assume that the A and B components have approximately equal brightness, which holds true at longer wavelengths (Delorme et al., 2013), then the A–b contrast can be expected to be ~ 5.7 mag.

For relative astrometry, we simply estimate the locations of the companion and the primary pair barycenter by eye, adopting a ± 1 pixel uncertainty. This gives a separation of 1.767 ± 0.014 arcsec and a position angle of 335.9 ± 0.5 deg. As can be seen in Fig. 3, the position in our Dec 2015 image is consistent with that in the Nov 2012 image of Delorme et al. (2013), and also confirms that orbital motion has occurred since their Oct 2002 epoch. Given the long baseline and relatively high proper motion of 2M0103, CPM is thoroughly obvious.

While a detailed analysis of the physical properties of 2M0103(AB)b is beyond the scope of this paper, it is interesting to assess whether the observational properties that we derive are consistent with the conclusions about the object properties in Delorme et al. (2013). In particular, we may ask whether our photometry is consistent with the ~ 12 – $14 M_{\text{Jup}}$ mass derived there. To test this, we first take the system age of 30 Myr adopted by Delorme et al. (2013) at face value, and use the BT-SETTL models (Baraffe et al., 2015) for an isochronal mass-brightness conversion. Given a primary mass of $\sim 0.2 M_{\text{sun}}$, the models predict $M_{z,A} = 8.3$ mag, and with an A–b contrast of 5.7 mag, this gives $M_{z,b} = 14.0$ mag, which in turn gives a mass prediction of 13–14 M_{Jup} from linear interpolation of public BT-SETTL grids. This is fully consistent with

the previous value derived for the system. Hence, the data give a consistent picture of a companion spectral energy distribution (SED) for a ~ 2000 K object, which at an age of 30 Myr corresponds to a mass in the range of the deuterium burning limit. However, a special note needs to be made about the age. The age assignment is based on THA membership in Delorme et al. (2013), so as a first check it is useful to test if we can support this conclusion. Our input sample classification for 2M0103 is THA, based on Kraus et al. (2014). We have re-assessed this membership using the BANYAN II tool, which supports this classification at a very high probability of 99.95%, so the membership indeed seems to be very robust. A remaining issue, then, is what age THA actually has. The 30 Myr adopted in Delorme et al. (2013) comes from Torres et al. (2008), but in this paper we have used the Bell et al. (2015) ages, which for THA gives a somewhat older age range of ~ 40 – 50 Myr. This corresponds to a BT-SETTL-predicted mass range of ~ 15 – $20 M_{\text{Jup}}$. Thus, we conclude that our data imply an SED consistent with the longer-wavelength data of Delorme et al. (2013), and that our analysis supports the classification of the system as a THA member, but we note that uncertainties in the specific age of THA broadens our error bars in mass relative to the discovery paper.

It is rather rare for such a planet-like object to be detected at such a short wavelength range as in z' -band. Fomalhaut b has been detected at yet shorter wavelengths (Kalas et al., 2008), but its observed flux does not arise from a photosphere (e.g. Janson et al., 2012b). H α emission related to accreting planets may have been observed in the LkCa 15 system (Sallum et al., 2015), but it remains unclear if the planets themselves have been imaged (Kraus & Ireland, 2012; Thalmann et al., 2016). It is all the more unusual considering the rather modest size of the 3.5m NTT. While the use of Lucky Imaging with Astralux was very useful in recovering this object, its detection is arguably less a question of instrumental capabilities than a question of target properties. It is the rare combination of proximity and youth that causes such a low-mass object as 2M0103(AB)b to be hot and luminous enough that it emits a non-negligible amount of radiation shortward of 1 μm . This underlines that studies of young moving groups with even modestly resource demanding instrument such as Astralux have the potential for yielding very low-mass discoveries. In this context, it also emphasizes the importance of following up the candidate companions yielded by the survey over longer timescales to test for CPM. While the faintest candidates in our survey are by far the most likely to be background contaminants, they are also potentially the most interesting individual objects provided by the survey.

4.3. Individual target notes

In this section, we make brief notes about a few targets that deserve or require particular attention.

J02303239-4342232: This system was already discussed in Sect. 4.1 due to the short estimated orbit of the AB pair. Here we additionally point out that there is a wide common proper motion companion at a separation of 173'' (Alonso-Floriano et al., 2015). Hence, the system is at least triple.

J02442137+1057411: The YMG membership of this star was classified as ambiguous in Malo et al. (2013), but

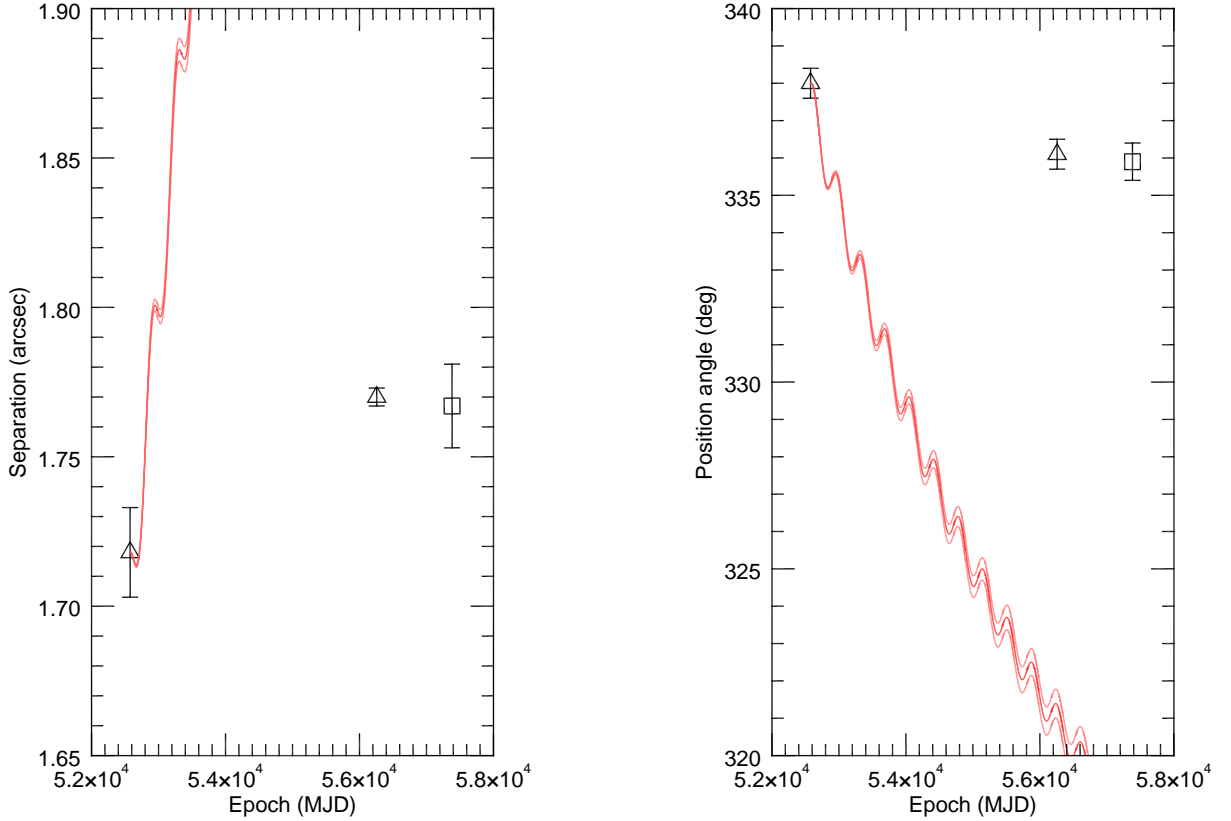


Fig. 3. Separation (left) and position angle (right) of 2M0103(AB)b relative to the AB barycenter as function of time. Triangles are data points from Delorme et al. (2013) and the square in each panel is the astrometry from our AstraLux image. Red lines correspond to the motion that 2M0103(AB)b would exhibit if it were a static background star, which can be firmly excluded. There is also significant orbital motion between the first epoch in 2002 and the later epochs.

since we observe it as being multiple, it is preferable with a more specific designation if that can be determined, for the age input to the mass estimation of the binary components. Hence, we used the BANYAN II tool to see if some clearer YMG preference could be derived. In this analysis, J02442137+1057411 was assigned a 93.4% probability of being a member of the β Pic moving group with the standard prior. We thus consider it as a bPMG member here.

J05015881+0958587: In addition to the wide component seen in the AstraLux images, which was originally reported in Henry et al. (1997) and confirmed in Delfosse et al. (1999), the primary in the system also has a spectroscopic binary companion (Delfosse et al., 1999). With a period of only 12 days, the spectroscopic pair is however significantly too close to be resolved in our images.

J05064991-2135091: Two of the three components of this system have individual 2MASS identifiers: J05064991-2135091 and J05064946-2135038. The latter has a close companion which is the third component of the system. We used the full AstraLux frame instead of subarray readout for this target, such that both wide components could be included.

J06153953-8433115: YMG membership of J06153953-8433115 is labelled as ‘ambiguous’ in Malo et al. (2013), but since we resolve it as a binary, it is desirable to attain a more detailed view of YMG membership for age and mass assignment purposes. This turns out to be a complicated issue for this target – BANYAN II gives only a 38.8% probability of bPMG membership versus 59.9% for the field with the standard priors. However, if we chose the priors to constrain the age to be <1 Gyr, the probability for bPMG membership goes up to 65.9%. The latter choice is arguably appropriate, since the star is part of the Riaz et al. (2006) sample which is indeed expected to be <1 Gyr. Hence, we adopt the bPMG age for this target, although we note that the evidence for such a membership is weak relative to most other targets in the survey.

J11211723-3446454: The two components of this system have individual 2MASS identifiers, J11211723-3446454 and J11211745-3446497. The full-frame field of view of AstraLux Sur was used to fit both components in simultaneously.

J14142141-1521215: In addition to the three components visible in the AstraLux field of view, there is a wide common proper motion companion at $65''$ re-

ported in e.g. Alonso-Floriano et al. (2015), with identifier 2MASS J14141700-1521125. This wide object happens to be part of the CASTOFFS survey (Schlieder et al., 2012, 2015, and Schlieder et al., in prep.) and thus has FEROS spectroscopy dedicated to it. The spectrum shows signs of high activity, with nearly all of the Balmer series in emission, and very broad lines ($v \sin i = 41 \pm 4$ km/s). This lends further support to the kinematic indication that the system is young. Exactly how young remains a factor of uncertainty – the classification of J14142141-1521215 in Malo et al. (2013) is for the β Pic moving group, but J14141700-1521125 fits better to the AB Dor YMG.

J15244849-4929473: J15244849-4929473 is single in the AstraLux field of view, but is noted as a single-line spectroscopic binary in Malo et al. (2014). Since no constraints are given on the orbital period, it cannot be assessed whether the unseen companion might become visible to AstraLux during some phase of its orbit.

J17165072-3007104: While this star was identified as a possible ambiguous YMG member in (Malo et al., 2013), our re-analysis with BANYAN II implies that this is a young field star with essentially no chance of being part of any of the identified YMGs, for any sensible choice of priors. For mass estimations of this resolved binary, we thus arbitrarily chose an age of 150 Myr, which is the upper end of the YMG ages used in this study.

J17243644-3152484: This is essentially an identical case as for J17165072-3007104 discussed above: Our BANYAN II re-analysis implies that this star is consistent with a young field star, but not possible to associate directly with any of the known young moving groups. As for J17165072-3007104, we use a tentative age of 150 Myr.

J18141047-3247344: Also known as V4046 Sgr, J18141047-3247344 is a double-lined spectroscopic binary with a period of 2.4 days (Quast et al., 2000). Furthermore, several studies (Kastner et al., 2011; Alonso-Floriano et al., 2015) have noted that it shares a common proper motion with J18142207-3246100, which is individually observed as a separate target in our survey. The separation between the two components is $169''$. Neither of these are however in the detectability range of AstraLux, in which no further companions are identified.

J19560294-3207186: The two stars J19560438-3207376 and J19560294-3207186, which were separately observed with AstraLux, form a wide binary pair with a separation of $26''$. As already noted in Bowler et al. (2015), J19560294-3207186 is itself a close pair, which we confirm in this survey. Furthermore, J19560294-3207186 is noted as a double-lined spectroscopic binary in Elliott et al. (2016), implying that there could be a third component in this close sub-system, and thus a component of a quadruple system in total. The system is part of the CASTOFFS survey, in which the spectroscopy in fact shows three distinct lines in both absorption as well as in emission ($H\alpha$ and Ca II H) for J19560294-3207186, supporting the quadruple nature of the system.

5. Summary and Conclusions

In this paper, we have presented high-resolution imaging observations of 181 late-type candidate members of nearby YMGs, with the purpose of identifying new binaries that can potentially be used for a range of calibration and age

determination purposes. We discovered 61 candidate companions, of which 23 were previously known and the other 38 are new detections. Of the previously known companions, the most notable object is 2M0103(AB)b, which was reported as a ~ 12 – $14 M_{\text{jup}}$ wide companion to a close pair of M-dwarfs (Delorme et al., 2013). Our analysis of the z' photometry acquired in this work supports the general conclusions in Delorme et al. (2013), but we note that the upper mass limit needs to be extended up to $20 M_{\text{jup}}$ when accounting for the full possible age range of the Tuc-Hor association quoted in the recent literature (Torres et al., 2008; Bell et al., 2015). Of the companions in total, 9 have estimated orbital periods less than 40 years, and are thus important targets for astrometric follow-ups to constrain their orbital motions.

We also used *Gaia* data from the recent TGAS release to re-analyze YMG membership for those targets that have new parallactic distances which weren't available in the original classifications of the targets. We find that in the majority of cases (17 of 29), the YMG could be confirmed with the new information. Still, in a significant fraction of cases (12 of 29), YMG membership was rejected with the new information. Hence, any individual YMG candidate member without a parallactic distance should be treated with a certain degree of caution. Over the next few years, *Gaia* will provide distances for all of the targets studied here, thus firmly identifying which systems are bona fide members and which are not. It is also likely to yield more YMG members that had previously been missed, and perhaps new nearby YMGs altogether. Finally, while the closest binaries resolved here will be too close to resolve with the much smaller *Gaia*, absolute astrometry of the unresolved system can still yield valuable constraints of the orbits when combined with resolved imaging from the ground.

Acknowledgements. M.J. gratefully acknowledges funding from the Knut and Alice Wallenberg Foundation. S.D. acknowledges support from the Northern Ireland Department of Education and Learning. The authors thank the ESO staff for their efficient support, S. Ciceri for transatlantic data transportation, and the anonymous referee for useful suggestions. This study made use of the CDS services SIMBAD and VizieR, the SAO/NASA ADS service, data from the ESA mission *Gaia*, and digitized archival data from the Anglo-Australian Observatory.

References

- Alonso-Floriano, F.J., Caballero, J., Cortes-Contreras, M., Solano, E., & Montes, D. 2015, *A&A* 583, 85
- Baraffe, I., Chabrier, G., Allard, F., & Hauschildt, P.H. 1998, *A&A* 337, 403
- Baraffe, I., Homeier, D., Allard, F., Chabrier, G. 2015, *A&A* 577, 42
- Bell, C.P.M., Mamajek, E.E., & Naylor, T. 2015, *MNRAS* 454, 593
- Bergfors, C., Brandner, W., Janson, M., et al. 2010, *A&A* 520, 54
- Biller, B.A., Liu, M.C., Wahhaj, Z., et al. 2013, *ApJ* 777, 160
- Bonavita, M., Desidera, S., Thalmann, C., Janson, M., Vigan, A., Chauvin, G., & Lannier, J. 2016, *A&A* 593, 38
- Bonnefoy, M., Chauvin, G., Dumas, C., et al. 2009, *A&A* 506, 799
- Bowler, B., Liu, M.C., Shkolnik, E.L., & Tamura, M. 2015, *ApJS* 216, 7
- Brandeker, A., Jayawardhana, R., Khavari, P., Haisch, K.E., & Mardones, D. 2006, *ApJ* 652, 1572
- Brandt, T.D., Kuzuhara, M., McElwain, M.W., et al. 2014, *ApJ* 786, 1
- Brown, A.G.A., Vallenari, A., Prusti, T., et al. 2016, *A&A special GAIA volume*
- Chauvin, G., Lagrange, A.-M., Bonavita, M. et al. 2010, *A&A* 509, 52
- Delfosse, X., Forveille, T., Udry, S., Beuzit, J.-L., Mayor, M., & Perrier, C. 1999, *A&A* 350, L39

- Delorme, P., Gagné, J., Girard, J.H. et al. 2013, *A&A* 553, L5
- Elliott, P., Huélamo, N., Bouy, H., et al. 2015, *A&A* 580, 88
- Elliott, P., Bayo, A., Melo, C.H.F., Torres, C.A.O., Sterzik, M.F., Quast, G.R., Montes, D. & Brahm, R. 2016, *A&A* 590, 13
- Gagné, J., Lafrenière, D., Doyon, R., Malo, L., & Artigau, É. 2014, *ApJ* 783, 121
- Gagné, J., Lafrenière, D., Doyon, R., Malo, L., & Artigau, É. 2015, *ApJ* 798, 73
- Henry, T.J., Ianna, P.A., Kirkpatrick, J.D., & Jahreiss, H. 1997, *AJ* 114, 388
- Hippler, S., Bergfors, C., Brandner, W., et al. 2009, *The Messenger* 137, 14
- Hormuth, F., Hippler, S., Brandner, W., Wagner, K., & Henning, T. 2008, *SPIE* 7104, 138
- Janson, M., Brandner, W., Lenzen, R., Close, L., Nielsen, E., Hartung, M., Henning, T., Bouy, H. 2007, *A&A* 462, 615
- Janson, M., Hormuth, F., Bergfors, C., et al. 2012, *ApJ* 754, 44
- Janson, M., Carson, J.C., Lafrenière, D., Spiegel, D.S., Bent, J.R., & Wong, P. 2012, *ApJ* 747, 116
- Janson, M., Bergfors, C., Brandner, W., et al. 2014, *ApJS* 214, 17
- Janson, M., Bergfors, C., Brandner, W., et al. 2014, *ApJ* 789, 102
- Jayawardhana, R. & Brandeker, A. 2001, *ApJ* 561, L111
- Kalas, P., Graham, J.R., Chiang, E. et al. 2008, *Science* 322, 1345
- Kastner, J.H., Sacco, G.G., Montez, R. et al. 2011, *ApJ* 740, L17
- Kraus, A.L. & Ireland, M. 2012, *ApJ* 745, 5
- Kraus, A.L., Shkolnik, E.L., Allers, K.N., & Liu, M.C. 2014, *AJ* 147, 146
- Köhler, R., Ratzka, T., Petr-Gotzens, M.G., & Correia, S. 2013, *A&A* 558, 80
- Kuzuhara, M., Tamura, M., Kudo, M. et al. 2013, *ApJ* 774, 11
- Lagrange, A.-M., Bonnefoy, M., Chauvin, G. et al. 2010, *Science*, 329, 57
- Law, N.M. 2006, Ph.D. thesis, Institute of Astronomy & Selwyn College, Cambridge University
- Malo, L., Doyon, R., Lafrenière, D., Artigau, E., Gagné, J., Baron, F., & Riedel, A. 2013, *ApJ* 762, 88
- Malo, L., Artigau, E., Doyon, R., Lafrenière, D., Albert, L., & Gagné, J. 2014, *ApJ* 788, 81
- Marois, C., Macintosh, B., Barman, T., Zuckerman, B., Song, I., Patience, J., Lafrenière, D., & Doyon, R. 2008, *Science*, 322, 1348
- Mason, B.D., Wycoff, G.L., Hartkopf, W.I., Douglass, G.G., & Worley, C.E. 2001, *AJ* 122, 3466
- McCaughrean, M.J. & Stauffer, J.R. 1994, *AJ* 108, 1382
- Michalik, D., Lindegren, L., & Hobbs, D. 2015, *A&A* 574, 115
- Montet, B.T., Bowler, B.P., Shkolnik, E.L., et al. 2015, *ApJ* 813, L11
- Montet, B.T., Morton, T.D., Foreman-Mackey, D., et al. 2015, *ApJ* 809, 25
- Perryman, M.A.C., Lindegren, L., Kovalevsky, J. et al. 1997, *A&A* 323, 49
- Quast, G.R., Torres, C.A.O., de la Reza, R. et al. 2000, *The Formation of Binary Stars*, ed. B. Reipurth & H. Zinnecker, IAU Symp. 200, 28
- Riaz, B., Gizis, J., & Harvin, J. 2006, *AJ* 132, 866
- Sallum, S., Follette, K., Eisner, J.A. et al. 2015, *Nature* 527, 342
- Schlieder, J.E., Lépine, S., & Michal, S. 2010, *AJ* 140, 119
- Schlieder, J.E., Lépine, S., & Michal, S. 2012, *AJ* 143, 80
- Schlieder, J.E., Herbst, T.M., Bonnefoy, M. et al. 2015, in 18th Cambridge Workshop on Cool Stars, Stellar Systems, and the Sun, ed. G. van Belle & H.C. Harris, 919
- Schlieder, J.E., Crossfield, I., Petigura, E. et al. 2016, *ApJ* 818, 87
- Skrutskie, M.F., Cutri, R.M., Stiening, R. et al. 2006, *AJ* 131, 1163
- Thalmann, C., Janson, M., Garufi, A. et al. 2016, *ApJ* 828, L17
- Torres, C.A.O., da Silva, L., Quast, G.R., de la Reza, R., & Jilinski, E. 2000, *AJ* 120, 1410
- Torres, C.A.O., da Silva, L., Melo, C.H.F., & Sterzik, M.F. 2008, in *Handbook of Star Forming Regions*, Vol. II, 757
- van der Marel, R.P., Gerssen, J., Guhathakurta, P., Peterson, R.C., & Gebhardt, K. 2002, *AJ* 124, 3255
- Zuckerman, B., Song, I., Bessell, M.S. & Webb, R.A. 2001, *ApJ* 562, L87

Table 1. Summary of the target sample.

2MASS ID	SpT	Assoc.	Ref ^a	J (mag)	δRA (mas/yr)	δDec (mas/yr)	d (pc)	Method ^b	Mult ^c
J00125703-7952073	M3.4	THA	K14	9.7	80.9	-46.1	48	Kin	1
J00144767-6003477	M3.5	THA	K14	9.7	91.3	-63.1	42	Kin	1
J00152752-6414545	M1.5	THA	K14	9.3	80.2	-49.9	50	Kin	1
J00172353-6645124	M2.5	bPMG	M14	8.56	104.3	-13.5	39	Plx	1
J00235732-5531435	M4.0	THA	K14	11.1	91.9	-66.9	42	Kin	1
J00273330-6157169	M3.5	THA	K14	10.3	87.5	-56.8	44	Kin	1
J00275023-3233060	M3.5	bPMG	M14	8.88	97.8	-60.9	32.3	Plx	1
J00302572-6236015	K7.9	THA	K14	8.4	95.5	-48.4	44	Kin	3
J00332438-5116433	M2.4	THA	K14	9.9	94.7	-59.9	42	Kin	1
J00340843+2523498	K7	ABMG	M14	8.48	83.4	-98.2	49	Kin	2
J00393579-3816584	M1.8	THA	K14	8.8	100.2	-65.5	40	Kin	1
J00421010-5444431	M3.0	THA	K14	9.8	89.4	-47.9	46	Kin	1
J00485254-6526330	M3.2	THA	K14	10.4	82.3	-40.7	50	Kin	1
J00514081-5913320	M4.1	THA	K14	11.3	98.0	-50.3	42	Kin	2
J01024375-6235344	M3.8	THA	K14	9.6	89.0	-39.6	46	Kin	2
J01033563-5515561	M5.1	THA	K14	10.2	100.3	-46.9	47.2	Plx	3
J01134031-5939346	M4.0	THA	K14	10.0	96.0	-35.4	44	Kin	1
J01211297-6117281	M4.1	THA	K14	11.3	80.7	-28.3	52	Kin	1
J01220441-3337036	K7	THA	GBII	8.31	110.1	-57.3	38.5	Plx	1
J01233280-4113110	M5.6	THA	K14	10.8	109.3	-54.8	38	Kin	1
J01275875-6032243	M4.0	THA	K14	11.1	88.4	-30.8	48	Kin	1
J01283025-4921094	M4.0	THA	K14	10.6	101.4	-41.7	42	Kin	1
J01372322+2657119	K5	GBII	M14	8.43	118.0	-128.0	37.6	Plx	1
J01372781-4558261	M5.4	THA	K14	11.1	116.0	-37.1	38	Kin	2
J01375879-5645447	M3.8	THA	K14	10.4	92.5	-32.8	46	Kin	1
J01484087-4830519	M1.5	ABMG	M14	9.19	111.2	-51.0	36	Kin	1
J01521830-5950168	M2-3	THA	M14	8.94	107.8	-27.0	40	Kin	1
J01540267-4040440	K7	COL	M14	9.78	50.3	-14.7	84	Kin	1
J02045317-5346162	K5	THA	M14	10.44	95.6	-30.9	42	Kin	1
J02125819-5851182	M3.5	THA	K14	9.3	88.4	-16.1	48	Kin	1
J02153328-5627175	M4.9	THA	K14	11.9	98.6	-29.3	42	Kin	1
J02180960-6657524	M4.5	THA	K14	10.8	99.0	-14.7	42	Kin	2
J02192210-3925225	M5.9	THA	K14	11.4	111.8	-44.0	36	Kin	1
J02303239-4342232	K5	COL	GBII	8.02	78.1	-7.6	48.5	Plx	2
J02341866-5128462	M4.2	THA	K14	10.6	100.6	-17.5	42	Kin	1
J02414683-5259523	K6	THA	GBII	7.58	97.8	-15.4	43.3	Plx	1
J02420204-5359147	M4.3	THA	K14	10.8	97.0	-20.8	42	Kin	1
J02423301-5739367	K5	THA	GBII	8.56	84.9	-9.2	48.5	Plx	1
J02442137+1057411	M0	BPMG	BII	7.97	68.4	-37.4	34.9	Plx	2
J02523096-1548357	M2.5	ABMG	M13	10.54	78.0	-92.0	42	Kin	1
J02553178-5702522	M4.4	THA	K14	11.1	89.5	-5.8	46	Kin	1
J02591904-5122341	M5.3	THA	K14	11.7	81.7	-14.7	48	Kin	1
J03050556-5317182	M5.1	THA	K14	11.1	89.4	-11.3	44	Kin	1
J03083950-3844363	M4.7	THA	K14	11.2	68.3	-11.0	58	Kin	1
J03093877-3014352	M4.7	THA	K14	11.6	88.7	-35.9	44	Kin	1
J03114544-4719501	M3.7	THA	K14	10.4	88.4	-4.0	44	Kin	1
J03190864-3507002	K7	THA	GBII	8.58	88.7	-20.0	45.3	Plx	1
J03241504-5901125	K7	COL	M14	9.55	37.8	10.5	90	Kin	2
J03291649-3702502	M3.7	THA	K14	10.6	89.8	-20.8	42	Kin	1
J03315564-4359135	K6	THA	GBII	8.3	88.7	-4.2	45.2	Plx	2
J03320347-5139550	M2	COL	M13	10.23	37.1	10.8	88	Kin	2
J03454058-7509121	M4	THA	M14	10.82	64.3	23.0	54	Kin	1
J03494535-6730350	K7	COL	M14	9.85	41.6	19.5	81	Kin	1
J03512287-5154582	M4.4	THA	K14	10.6	71.9	2.4	50	Kin	1
J03561624-3915219	M4.5	THA	K14	10.5	68.6	-3.7	52	Kin	2
J04013874-3127472	M4.7	THA	K14	12.0	59.3	-12.3	58	Kin	1
J04074372-6825111	M2.6	THA	K14	10.4	57.8	22.0	60	Kin	1
J04082685-7844471	M0	CAR	M14	9.28	55.7	42.8	53	Kin	1
J04091413-4008019	M3.5	COL	M14	10.65	46.4	8.1	63	Kin	1
J04133314-5231586	M1.7	THA	K14	10.0	65.7	14.8	50	Kin	1
J04133609-4413325	M3.3	THA	K14	10.8	56.7	0.4	60	Kin	1
J04274963-3327010	M4.5	THA	K14	11.2	61.8	-0.7	52	Kin	1
J04363294-7851021	M4	ABMG	M14	10.98	32.8	47.4	56	Kin	1
J04435860-3643188	M3.5	THA	K14	10.7	54.1	-2.1	55	Kin	1
J04440099-6624036	M0.5	THA	M14	9.47	53.0	30.2	55	Kin	1
J04470041-5134405	M2.4	THA	K14	10.1	54.9	14.4	55	Kin	1
J04475779-5035200	M4.1	THA	K14	10.9	47.9	17.8	60	Kin	2
J04480066-5041255	K7	THA	GBII	8.74	56.9	17.1	57.7	Plx	2
J04514615-2400087	M3	ABMG	M13	10.56	41.8	-56.9	45	Kin	1
J04515303-4647309	M0	COL	M14	9.8	29.0	14.5	76	Kin	1
J04554034-1917553	M0.5	ABMG	M14	9.78	21.8	-66.1	49	Kin	1
J05015881+0958587	M3	bPMG	M13	7.21	12.1	-74.4	24.9	Plx	2
J05064991-2135091	M1+M3.5+M4	bPMG	GBII	7.05	46.6	-16.3	19.7	Plx	3
J05111098-4903597	M3.5	COL	M14	10.64	33.0	20.4	62	Kin	2
J05142736-1514514	M3.5	COL	M14	10.71	36.0	-16.0	63	Kin	2
J05142878-1514546	M3.5	COL	M14	10.95	34.1	-14.2	58	Kin	1
J05164586-5410168	M3	COL	M14	10.43	26.3	26.6	69	Kin	1
J05224571-3917062	K7	FLD	GBII	8.31	0.3	6.0	213.2	Plx	1
J05240991-4223054	M0.5	ABMG	M14	10.58	4.9	-13.3	52	Kin	2
J05332558-5117131	K7	FLD	GBII	8.99	42.2	27.0	55.2	Plx	1
J05395494-1307598	M3	COL	M14	10.6	26.4	-18.9	54	Kin	1
J05432676-3025129	M0.5	COL	M14	10.41	11.6	-0.3	87	Kin	1
J06012186-1937547	M3.5	COL	M13	11.37	10.4	-9.0	79	Kin	1

Table 1. continued.

2MASS ID	SpT	Assoc.	Ref ^a	J (mag)	δ RA (mas/yr)	δ Dec (mas/yr)	d (pc)	Method ^b	Mult ^c
J06135773-2723550	K5	FLD	GBII	9.74	1.2	4.8	369	Plx	1
J06153953-8433115	M3	bPMG	BII	9.25	-32.2	107.0	31	Kin	2
J06475229-2523304	K7	Amb	M13	8.35	22.4	-70.3	240	Spec	2
J06511418-4037510	K5	FLD	GBII	8.17	-1.0	7.1	1492	Plx	1
J07170438-6311123	M2	Amb	M13	9.73	-13.1	48.0	53	Spec	1
J07343426-2401353	M3.5	ARG	M13	10.65	-22.0	30.0	71	Kin	2
J07523324-6436308	K7	CAR	M14	9.7	-5.9	27.8	88	Kin	3
J07540718-6320149	M3	CAR	M14	10.33	-10.8	30.0	80	Kin	2
J08083927-3605017	K7	COL	M14	9.53	-7.2	8.4	90	Kin	2
J08173829-6817162	M3.8	CAR	G15	10.36	-15.6	58.1	53	Kin	2
J08173943-8243298	M4	bPMG	M14	7.47	-81.9	102.6	27	Kin	2
J08422284-8345248	K7	CAR	M13	9.45	-49.5	91.2	41	Kin	1
J08465879-7246588	K7	FLD	GBII	8.49	-71.5	56.3	45.4	Plx	1
J09032434-6348330	M0.5	CAR	M14	9.57	-34.5	35.4	66	Kin	3
J09331427-4848331	K7	FLD	GBII	8.94	-48.9	19.6	45.5	Plx	1
J09353126-2802552	K7	Amb	M13	8.51	-49.4	-57.4	46	Spec	1
J10120908-3124451	M4	TWA	M14	8.85	-74.8	-9.4	53.9	Plx	2
J10182870-3150029	M0	Amb	GBII	8.87	-55.6	-19.5	63.9	Plx	1
J10252092-4241539	M1	Amb	M14	9.5	-46.8	-2.2	58	Kin	1
J10585054-2346206	M3.8	Amb	G15	10.3	-92.3	-15.5	42	Kin	1
J11112820-2655027	M3.8	TWA	G15	10.33	-87.4	-29.7	43	Kin	1
J11132622-4523427	M0	TWA	M14	9.41	-44.1	-8.1	96.2	Plx	1
J11210549-3845163	M1	TWA	M13	9	-68.3	-12.1	52	Kin	1
J11211723-3446454	M1	TWA	M14	8.43	-67.4	-17.0	55.6	Plx	2
J11321831-3019518	M5	TWA	M14	9.64	-89.6	-25.8	46	Kin	1
J11393382-3040002	M3.9	TWA	G15	9.98	-79.9	-30.0	48	Kin	1
J11455177-5520456	K5	FLD	GBII	8.02	-99.6	-5.9	42.6	Plx	1
J12072738-3247002	M3	TWA	M14	8.62	-72.7	-29.3	53.8	Plx	1
J12092998-7505400	M3	ARG	M14	9.91	-65.3	-0.6	77	Kin	2
J12103101-7507205	M4	Amb	M13	11.19	-66.5	-5.8	28	Spec	1
J12153072-3948426	M1	TWA	GBII	8.17	-76.5	-26.7	51.8	Plx	1
J12170465-5743558	K7	FLD	GBII	8.71	-90.3	-11.3	231	Plx	1
J12242443-5339088	M5	Amb	M13	10.51	-180.0	-60.0	16	Spec	1
J12313807-4558593	M3	TWA	M14	9.33	-64.4	-28.6	77.5	Plx	1
J13213722-4421518	M0.5	Amb	M13	9.74	-34.9	-18.8	64	Spec	1
J13412668-4341522	M3.5	Amb	M14	10.75	-107.0	-60.8	42	Kin	1
J13545390-7121476	M2.5	bPMG	M14	8.55	-165.0	-132.7	21	Kin	1
J13591045-1950034	M4.5	ARG	M13	8.33	-552.7	-183.1	10.7	Plx	1
J14142141-1521215	K5	bPMG	M13	7.43	-199.9	-172.8	30.2	Plx	3
J14252913-4113323	M2.5	Amb	M14	8.55	-46.8	-49.2	66.9	Plx	1
J14284804-7430205	M1	ARG	M13	9.26	-62.2	-36.3	76	Kin	1
J14563812-6623419	M1.5	ARG	M13	10.4	-60.9	-40.4	73	Kin	1
J15163224-5855237	K7	ARG	M13	9.1	-42.8	-44.2	77	Kin	2
J15244849-4929473	M2	ABMG	M14	8.16	-121.1	-238.9	23	Kin	1
J16074132-1103073	M4	ABMG	M14	9.82	-64.0	-148.0	36	Kin	2
J16572029-5343316	M3	bPMG	GBII	8.69	-21.3	-90.9	51.5	Plx	3
J17080882-6936186	M3.5	THA	M14	9.06	-55.6	-80.2	49	Kin	2
J17115853-2530585	M1	ARG	M13	9.9	-15.1	-34.0	65	Kin	1
J17130733-8552105	M0	THA	M14	8.59	-35.2	-58.1	62	Kin	2
J17150219-3333398	M0	bPMG	M14	7.92	7.6	-176.9	23	Kin	1
J17165072-3007104	M2.5	FLD	BII	10.37	-8.0	-36.0	65	Spec	2
J17243644-3152484	K7	FLD	BII	9	-7.0	-34.6	56	Spec	3
J17275761-4016243	M4	Amb	M13	10.04	-13.1	-50.4	43	Spec	1
J17292067-5014529	M3	bPMG	M14	8.87	-6.3	-63.5	64	Kin	2
J17300060-1840132	M3.5	Amb	M13	9.92	-8.1	-39.3	45	Spec	1
J17580616-2222238	M1	Amb	M13	9.72	-5.9	-44.1	61	Spec	1
J18141047-3247344	K6	Amb	M14	8.07	3.3	-52.0	73	Kin	1
J18142207-3246100	M1.5	bPMG	M14	9.44	7.3	-39.9	90	Kin	1
J18151564-4927472	M3	bPMG	M14	8.92	8.3	-71.5	61	Kin	1
J18202275-1011131	K5+K7	bPMG	M14	7.64	10.5	-33.9	61	Kin	2
J18420694-5554254	M3.5	bPMG	M14	9.49	11.2	-81.4	54	Kin	1
J18450097-1409053	M5	ARG	M14	8.47	46.0	-84.0	16	Kin	2
J18465255-6210366	M1	bPMG	M14	8.75	14.6	-81.1	54	Kin	1
J18504448-3147472	K7	bPMG	GBII	8.31	13.7	-75.7	49.7	Plx	1
J18553176-1622495	M0.5	ABMG	M13	9.13	32.6	-175.6	34	Kin	1
J18580415-2953045	M0	FLD	GBII	8.86	8.4	-54.1	78.3	Plx	1
J19102820-2319486	M4	bPMG	M14	9.1	17.6	-51.6	67	Kin	2
J19225071-6310581	M3	THA	M14	9.45	-10.7	-77.4	61	Kin	1
J19233820-4606316	M0	bPMG	M14	9.11	17.9	-57.9	70	Kin	1
J19243494-3442392	M4	bPMG	M14	9.67	23.2	-72.1	54	Kin	1
J19312434-2134226	M2.5	ARG	M14	8.69	63.0	-110.1	26	Plx	1
J19420065-2104051	M3.5	ABMG	M13	8.69	48.0	-276.0	21	Kin	1
J19560294-3207186	M4	bPMG	M14	8.96	32.6	-61.0	55	Kin	2
J19560438-3207376	M0	bPMG	GBII	8.71	32.6	-68.9	50.2	Plx	1
J20013718-3313139	M1	bPMG	M14	9.15	27.1	-60.9	61	Kin	1
J20072376-5147272	K6	ARG	GBII	8.16	87.7	-143.6	33.7	Plx	1
J20220177-3653014	M4.5	ABMG	M13	10.71	72.0	-188.0	33	Kin	1
J20223306-2927499	M3.5	ABMG	M13	10.41	32.0	-104.0	58	Kin	2
J20330186-4903105	M5.2	bPMG	G15	10.11	115.1	-208.0	16.3	Kin	1
J20333759-2556521	M4.5	bPMG	M14	9.71	51.8	-76.8	48.3	Plx	1
J20395460+0620118	K7	FLD	GBII	7.92	93.0	-103.3	38	Plx	1
J20405616-8245093	M3.6	ARG	G15	9.52	89.9	-124.3	33	Kin	1
J20560274-1710538	K7+M0	bPMG	M14	7.85	59.3	-63.0	44	Kin	2

Table 1. continued.

2MASS ID	SpT	Assoc.	Ref ^a	J (mag)	δ RA (mas/yr)	δ Dec (mas/yr)	d (pc)	Method ^b	Mult ^c
J21100535-1919573	M2	bPMG	M14	8.11	88.6	-92.5	32	Kin	1
J21103096-2710513	M5	bPMG	M13	11.2	60.3	-79.7	40	Kin	1
J21130526-1729126	K6	ABMG	GBII	8.35	76.9	-147.6	37.2	Plx	1
J21212873-6655063	K7	bPMG	GBII	7.88	116.3	-90.9	32.1	Plx	1
J21334415-3453372	M1.5	Amb	M13	10.24	40.4	-72.5	69	Spec	1
J21342935-1840372	M4	ARG	M13	10.05	79.0	-11.4	51	Kin	2
J21370885-6036054	M3	THA	M14	9.64	41.3	-91.3	48	Kin	1
J22440873-5413183	M4	THA	M14	9.36	70.9	-60.1	49	Kin	2
J22470872-6920447	K6	FLD	GBII	8.89	66.2	-65.8	52	Plx	1
J23124644-5049240	M4.4	THA	K14	9.1	77.6	-75.7	46	Kin	2
J23204705-6723209	M5	THA	M14	9.99	80.0	-97.1	41	Kin	2
J23301341-2023271	M3	FLD	GBII	7.2	313.9	-204.6	16.1	Plx	1
J23332198-1240072	K5	ARG	M13	10.28	164.2	9.0	31	Kin	2
J23424333-6224564	M4.4	THA	K14	11.3	80.9	-61.6	46	Kin	1
J23524562-5229593	M5.3	THA	K14	11.6	76.4	-82.4	44	Kin	1

^aReference for the association allocation. BII: Re-evaluation in this work with BANYANII, based on ambiguous classification in previous works. GBII: Re-evaluation based on GAIA data. G15: Gagné et al. (2015). K14: Kraus et al. (2014). M13: Malo et al. (2013). M14: Malo et al. (2014).

^bMethod of distance estimation. Plx: Parallax. Kin: Kinematics. Spec: Spectroscopic.

^cThe number of components seen in the AstraLux images (i.e. 1 is single, etc).

Table 2. Astrometric properties.

2MASS ID	Pair	ρ ($''$)	θ (deg)	Epoch (yr)	CPM ^a	Ref ^b
J00302572-6236015	AB ^c	0.098±0.005	262.4±0.6	2015.99	I	TP
J00302572-6236015	AC	4.413±0.023	238.8±0.2	2015.99	Y	TP
J00340843+2523498	AB	1.523±0.009	102.5±0.2	2015.91	Y	WDS
J00514081-5913320	AB	10.990±0.052	260.2±0.2	2015.99	N	TP
J01024375-6235344	AB	0.671±0.003	325.5±0.2	2015.99	I	TP
J01033563-5515561	AB ^c	0.192±0.001	56.9±0.4	2015.98	Y	D13
J01033563-5515561	AB-C	1.767±0.014	335.9±0.5	2015.98	Y	D13
J01372781-4558261	AB	0.147±0.003	299.7±1.1	2015.99	I	TP
J02180960-6657524	AB ^c	0.306±0.002	346.1±0.2	2015.99	I	TP
J02303239-4342232	AB	0.097±0.001	212.5±1.2	2015.98	Y	E15
J02442137+1057411	AB	0.249±0.002	322.6±0.2	2015.91	I	TP
J03241504-5901125	AB	0.477±0.008	280.7±0.3	2015.98	U	N/A
J03315564-4359135	AB	0.400±0.006	94.6±0.3	2015.99	Y	E15
J03320347-5139550	AB	3.171±0.018	115.7±0.2	2015.98	U	N/A
J03561624-3915219	AB	0.274±0.003	107.9±0.2	2015.99	U	N/A
J04475779-5035200	AB ^c	0.530±0.002	121.4±0.2	2015.91	U	N/A
J04480066-5041255	AB	1.047±0.011	345.4±0.2	2015.98	Y	E15
J05015881+0958587	AB	1.398±0.012	146.9±0.2	2015.98	Y	D99
J05064991-2135091	AB	8.454±0.039	307.0±0.2	2015.99	Y	WDS
J05064991-2135091	BC	0.966±0.008	112.8±0.2	2015.99	Y	WDS
J05111098-4903597	AB	2.397±0.017	168.2±0.2	2015.99	U	N/A
J05142736-1514514	AB	2.679±0.016	268.5±0.2	2015.98	U	N/A
J05240991-4223054	AB	0.225±0.005	61.1±0.4	2015.98	U	N/A
J06153953-8433115	AB	0.965±0.008	275.5±0.2	2015.98	I	TP
J06153953-8433115	AB	0.974±0.008	275.4±0.2	2015.99	I	TP
J06475229-2523304	AB	1.076±0.013	27.9±0.2	2015.99	Y	WDS
J07343426-2401353	AB	0.579±0.003	127.1±0.2	2015.99	U	N/A
J07343426-2401353	AB	0.580±0.003	127.1±0.2	2016.38	U	N/A
J07523324-6436308	AB	1.425±0.012	211.0±0.2	2015.98	U	N/A
J07523324-6436308	BC	0.151±0.002	330.1±0.7	2015.98	U	N/A
J07523324-6436308	AB	1.440±0.012	210.6±0.2	2016.38	U	N/A
J07523324-6436308	BC	0.162±0.001	329.9±0.7	2016.38	U	N/A
J07540718-6320149	AB	0.854±0.011	156.8±0.2	2015.98	U	N/A
J07540718-6320149	AB	0.859±0.004	156.6±0.2	2016.38	U	N/A
J08083927-3605017	AB	0.108±0.001	309.4±0.8	2015.99	U	N/A
J08083927-3605017	AB	0.104±0.001	305.5±0.4	2016.38	U	N/A
J08173829-6817162	AB	1.585±0.012	39.4±0.2	2016.38	U	N/A
J08173943-8243298	AB	0.584±0.003	3.8±0.2	2015.98	Y	C10
J08173943-8243298	AB	0.584±0.003	3.6±0.2	2016.38	Y	C10
J09032434-6348330	AC	7.986±0.038	153.3±0.2	2015.98	U	N/A
J09032434-6348330	AB	1.113±0.011	66.0±0.2	2015.98	U	N/A
J09032434-6348330	AB	1.139±0.012	67.3±0.2	2016.38	U	N/A
J10120908-3124451	AB	1.040±0.012	87.2±0.2	2015.98	Y	WDS
J10120908-3124451	AB	1.037±0.011	86.9±0.2	2016.38	Y	WDS
J11211723-3446454	AB	5.049±0.025	327.3±0.2	2015.98	Y	WDS
J12092998-7505400	AB ^c	0.300±0.002	169.1±0.4	2015.99	Y	TP
J12092998-7505400	AB	0.297±0.002	169.5±0.2	2016.38	Y	TP
J14142141-1521215	AB	0.244±0.002	164.0±0.7	2016.38	Y	C10
J14142141-1521215	AC	1.565±0.012	78.8±0.2	2016.38	Y	C10
J15163224-5855237	AB	2.331±0.014	27.0±0.2	2016.38	U	N/A
J16074132-1103073	AB	0.740±0.011	149.2±0.2	2016.38	Y	B15
J16572029-5343316	AB	3.196±0.013	101.5±0.2	2016.38	U	N/A
J16572029-5343316	AC	3.487±0.014	298.4±0.2	2016.38	U	N/A
J17080882-6936186	AB	0.441±0.002	9.3±0.2	2016.38	I	TP
J17130733-8552105	AB ^c	0.360±0.003	114.5±0.2	2016.38	U	N/A

Table 2. continued.

2MASS ID	Pair	ρ ($''$)	θ (deg)	Epoch (yr)	CPM ^a	Ref ^b
J17165072-3007104	AB	1.701±0.012	298.7±0.2	2016.38	U	N/A
J17243644-3152484	AB	0.142±0.001	351.8±1.8	2016.38	U	N/A
J17243644-3152484	AC	0.902±0.011	198.2±0.2	2016.38	U	N/A
J17292067-5014529	AB	0.686±0.010	15.7±0.2	2016.38	Y	E15
J18202275-1011131	AB	0.998±0.011	17.7±0.2	2016.38	Y	WDS
J18450097-1409053	AB	3.224±0.016	123.8±0.2	2016.38	Y	TP
J19102820-2319486	AB	0.424±0.002	172.8±0.2	2016.38	U	N/A
J19560294-3207186	AB	0.177±0.001	250.7±0.2	2016.38	Y	B15
J20223306-2927499	AB ^c	0.156±0.001	214.2±2.0	2016.38	I	TP
J20560274-1710538	AB	2.181±0.013	140.3±0.2	2016.38	Y	J01
J21342935-1840372	AB ^c	0.334±0.006	270.0±0.4	2016.38	I	TP
J22440873-5413183	AB	0.517±0.003	298.3±0.2	2015.99	Y	C10
J23124644-5049240	AB	0.426±0.003	71.4±0.2	2015.99	I	TP
J23204705-6723209	AB	2.870±0.017	15.2±0.2	2015.99	Y	TP
J23332198-1240072	AB	3.767±0.022	14.6±0.2	2015.99	N	TP

^aFlag for CPM. Y if proven CPM, N if non-CPM, U if undetermined, I if implied (see text).

^bCPM reference. TP: This paper. WDS: The Washington Double Star catalogue (Mason et al., 2001). B15: Bowler et al. (2015). C10: Chauvin et al. (2010). D99: (Delfosse et al., 1999). D13: (Delorme et al., 2013). E15: Elliott et al. (2015). J01: Jayawardhana & Brandeker (2001).

^cPair displays false triple effect – possibly subject to a 180 deg ambiguity.

Table 3. Photometric and derived properties.

2MASS ID	Pair	$\Delta z'$ (mag)	m_1 (M_{sun})	m_2 (M_{sun})	a (AU)	P_{est} (yr)
J00302572-6236015	AC	1.33±0.02	0.6	0.6	194	2470
J00340843+2523498	AB	0.04±0.01	0.6	0.6	75	589
J00514081-5913320	AB	2.35±0.04	0.13	0.03	462	24792
J01024375-6235344	AB	0.56±0.02	0.4	0.3	31	205
J01372781-4558261	AB	1.30±0.05	0.11	0.06	6	32
J02180960-6657524	AB	0.76±0.02	0.15	0.1	13	92
J02442137+1057411	AB	2.03±0.05	0.7	0.2	9	27
J03241504-5901125	AB	2.97±0.13	0.8	0.2	43	281
J03315564-4359135	AB	4.09±0.27	0.7	0.08	18	87
J03320347-5139550	AB	1.57±0.02	0.6	0.3	279	4914
J03561624-3915219	AB	1.00±0.01	0.3	0.15	14	80
J04480066-5041255	AB	0.92±0.02	0.7	0.5	60	429
J05015881+0958587	AB	0.79±0.02	0.6	0.4	35	205
J05064991-2135091	AB	0.49±0.01	0.6	0.5	162	1972
J05064991-2135091	BC	0.53±0.01	0.5	0.4	19	84
J05111098-4903597	AB	6.10±0.07	0.3	0.015	149	3228
J05142736-1514514	AB	1.26±0.02	0.3	0.13	169	3344
J05240991-4223054	AB	1.33±0.03	0.4	0.2	12	52
J06153953-8433115	AB	0.13±0.01	0.17	0.15	30	289
J06475229-2523304	AB	3.22±0.05	1.4	0.7	258	2864
J07343426-2401353	AB	0.37±0.01	0.3	0.2	41	373
J07523324-6436308	AB	2.41±0.03	0.7	0.2	125	1480
J07523324-6436308	BC	0.40±0.06	0.2	0.17	13	80
J07540718-6320149	AB	0.28±0.02	0.5	0.4	68	595
J08083927-3605017	AB	1.39±0.06	0.7	0.4	10	29
J08173829-6817162	AB	0.53±0.03	0.3	0.2	84	1089
J08173943-8243298	AB	0.83±0.02	0.5	0.3	16	70
J09032434-6348330	AB	2.37±0.02	0.6	0.15	73	727
J09032434-6348330	AC	1.64±0.03	0.6	0.2	527	13529
J10120908-3124451	AB	0.01±0.04	0.3	0.3	56	542
J11211723-3446454	AB	0.00±0.02	0.7	0.7	281	3975
J14142141-1521215	AB	3.03±0.21	0.8	0.15	7	21
J14142141-1521215	AC	1.32±0.03	0.8	0.5	47	285
J15163224-5855237	AB	0.00±0.03	0.7	0.7	179	2032
J16074132-1103073	AB	0.08±0.03	0.3	0.3	27	178
J16572029-5343316	AB	5.60±0.36	0.7	0.03	165	2471
J16572029-5343316	AC	6.59±0.69	0.7	0.02	180	2836
J17080882-6936186	AB	1.09±0.05	0.6	0.3	22	106
J17165072-3007104	AB	0.99±0.02	0.5	0.3	111	1300
J17243644-3152484	AB	2.29±0.09	0.7	0.4	8	21
J17243644-3152484	AC	0.17±0.02	0.7	0.7	51	303
J17292067-5014529	AB	0.18±0.02	0.6	0.6	44	266
J18202275-1011131	AB	0.35±0.02	0.9	0.8	61	364
J18450097-1409053	AB	0.11±0.02	0.2	0.2	52	586
J19102820-2319486	AB	0.83±0.03	0.7	0.5	28	138
J19560294-3207186	AB	1.71±0.04	0.6	0.2	10	34
J20560274-1710538	AB	2.08±0.02	0.8	0.3	96	896
J22440873-5413183	AB	0.40±0.01	0.4	0.3	25	152
J23124644-5049240	AB	0.54±0.02	0.5	0.4	20	91
J23204705-6723209	AB	1.09±0.02	0.3	0.15	118	1903
J23332198-1240072	AB	6.60±0.08	0.3	0.02	117	2231